



Contents lists available at ScienceDirect

Journal of King Saud University – Science

journal homepage: www.sciencedirect.com

Original article

Recent advances in chemically and biologically synthesized nanostructures for colorimetric detection of heavy metal

Tahir Rasheed^{a,*}, Sameera Shafi^b, Jazib Ali^c, Farooq Sher^d, Komal Rizwan^e, Salahuddin Khan^f^a Interdisciplinary Research Center for Advanced Materials, King Fahd University of Petroleum and Minerals (KFUPM), Dhahran 31261, Saudi Arabia^b Institute of Chemistry, The Islamia University of Bahawalpur, Bahawalnagar Campus 62300, Pakistan^c Electronic Engineering Department, University of Rome Tor Vergata, Italy^d Department of Engineering, School of Science and Technology, Nottingham Trent University, Nottingham NG11 8NS, United Kingdom^e Department of Chemistry, University of Sahiwal, Sahiwal 57000, Pakistan^f College of Engineering, King Saud University, P.O. Box 800, Riyadh 11421, Saudi Arabia

ARTICLE INFO

Article history:

Received 12 July 2021

Revised 12 November 2021

Accepted 28 November 2021

Available online 01 December 2021

Keywords:

Nanomaterials

Heavy metals

Colorimetric detection

Chemical and biological synthesis

ABSTRACT

The ecological system is being threatened by the environmental risks related to soil and water pollution. The ecological integrity and environmental quality mandate the approaches and efforts to ensure safer monitoring of health system. A number of technologically advanced methodologies have been ameliorating the impact of toxic chemicals and heavy metals pollutants in the environment. In this regard, the colorimetric monitoring of heavy metal based analytes have extensively been investigated in a variety of fields including, environmental science biomedicine and food industry. Their wide range of applications owes from their ability to offer detection of these analytes with bare eye, high selectivity and sensitivity, facile synthesis and easy operating conditions. Herein, the recent advancement in the field of colorimetric detection based on chemically and biologically synthesized nanomaterials has been reviewed. Emerging biologically synthesized nanomaterials via eco-friendlier green routes and chemically synthesized nanomaterials offers a number of desirable features for the detection of target analyte.

© 2021 The Authors. Published by Elsevier B.V. on behalf of King Saud University. This is an open access article under the CC BY-NC-ND license (<http://creativecommons.org/licenses/by-nc-nd/4.0/>).

1. Introduction

Nowadays, environmental contamination presents complexity and diversity, with countless harmful pollutants from anthropogenic sources which are polluting the environment severely (Lin et al., 2014; Sarkar et al., 2018; Rasheed and Nabeel, 2019; Nabeel and Rasheed, 2020; Azmi et al., 2013; Azmi et al., 2016; Azmi et al., 2020). With increased agricultural growth and industrial developments, a number of new chemicals, such as harmful compounds, materials and elements have been discharged into air, water and soil. The indiscriminating use of pesticide and veterinary drugs, release of industrial waste into water bodies, the unrestricted usage of dangerous substances in different products

of consumer use are the main sources of environmental pollution. A significant number of chemicals and disinfectants were utilized everywhere in 2020, particularly through the pandemic prevention of the new coronavirus (COVID-19). Not only chemicals and disinfectants posing the threat to the biological environment, but multifaceted secondary compounds might also posture health hazards. To assess their health impacts and environmental risks, the development of new analytical methodologies is of urgent need. At present, a number of sophisticated techniques are implemented for the detection of pollutants such as gas chromatography-triple quadrupole mass spectrometry (GC-MS), liquid chromatography-tandem quadrupole mass spectrometry (LC-MS), inductively coupled plasma-mass spectrometry (ICP-MS), and others (Gaiss et al., 2019; Kanwar et al., 2020; St-Jean et al., 2019; Yao et al., 2012; Zhang et al., 2020; Zhang et al., 2017; Zhao et al., 2018). Undoubtedly, these techniques can measure and detect these contaminants with greater efficacy, but the main disadvantage of these techniques are the requirement of skilled individuals, expensive instrumentation and complex operating conditions limit their usefulness. On contrary, because of its simplicity, cost friendly and excellent performance, the use of colorimetric detection approach has gained the attention of an scientists (Boruah and Das, 2020;

* Corresponding author.

E-mail addresses: tahir.rasheed@hotmail.com, tahir.rasheed@kfupm.edu.sa (T. Rasheed).

Peer review under responsibility of King Saud University.



Production and hosting by Elsevier

<https://doi.org/10.1016/j.jksus.2021.101745>

1018-3647/© 2021 The Authors. Published by Elsevier B.V. on behalf of King Saud University.

This is an open access article under the CC BY-NC-ND license (<http://creativecommons.org/licenses/by-nc-nd/4.0/>).

Rasheed et al., 2020; Rasheed et al., 2018a; Rasheed et al., 2018b; Rasheed et al., 2018c; Rasheed et al., 2019a).

Due to great catalytic potential, great reactivity, strong adsorption potential, and greater surface area, nanomaterial based colorimetric sensors have presented considerable promise in detection of heavy metals during recent years. Various nanomaterials including, polymer based nanomaterials, metal/metal oxide nanoparticles, carbon and silicon based nanomaterials have been employed to construct the distinctive type of colorimetric sensors for sensing of heavy metal ions (Rasheed et al., 2019b; Rasheed et al., 2019c). The improved selectivity and sensitivity of colorimetric nanosensor is originated from their high degree of functionalization, greater volume-to-surface ratio, size-dependent features and high reactivity (Borah et al., 2015). In addition, anchoring of organic ligand, covalent functionalization, and nanocomposite fabrication have greater impact on the enhanced sensitivity and selectivity in recognition of heavy metal ions. Further, introduction of nanomaterials has greatly improved the reproducibility of the colorimetric nano sensors as well as the lower limit of detection for determining the heavy metal ions (Kaur et al., 2015). The optical and electrical characteristics of nanomaterials are generally taken into account in this context. Herein, we have attempted to present the documented reports based on use of different nanomaterials as colorimetric sensors for colorimetric recognition of heavy metal ions. This review covers the application of biologically and chemically synthesized nanomaterials for detection of heavy metal ions visually. Additionally, this review deals with the lingering challenges and future perspectives in utilizing these nanomaterials for colorimetric recognition of heavy metal ions are addressed.

2. Distribution of heavy metal pollution in soil

It is difficult to detect heavy metals in soil which act as a pollutant (García-Carmona et al., 2017; Rahman et al., 2006). Heavy metals in the soil have a wide range of three-dimensional changeability due to the effect of a huge number of pollution sources which ultimately differs the properties of the soil heavy metals. This change can show the nature of their source and higher level of pollution cause by them. Hence, for the soil pollution inhibition and its control along with some prior awareness regarding soil environmental dangers, there should be some scientific study on the nature of soil and wide range spreading of the elements i.e. heavy metals (Trujillo-González et al., 2016). Geostatistics is considered to be one of the most appropriate way to study and calculate the spatial distributional features of the heavy metals along with their altering trends. Moreover, it includes collection of data from particular area with the help of spatial exclamation, which gives impartial optimized assessment to study the soil with heavy metals with their spatial inside distribution, which helps to describe the pollution mechanism up to a certain level. In different studies (Jang et al., 2007; Ghadermazi et al., 2011) Kelepertzis (Kelepertzis, 2014) multivariate statistical way was used with the combination of GIS technology to study the main cause of the heavy metals chain by doing soil surveys sample plots by using Argolida Basin, Peloponnese, Greece in the agricultural system followed by the map making of these heavy metals present in the mud with their spatial distribution as shown in Fig. 1 which describes the dangerous zone of pollution. So, there should be focus on pollutants of the particular environment, by different control methods. But fitting geostatistics reveals that those areas with high level of pollutant are excluded from the spatial prediction. Spatial autocorrelation analysis removes this error and detect the spatial clustering and spatial outliers of the soil with high content of heavy metal.

Heavy metals content of the soil can be displayed directly by combining the data with graphic processing with the help of GIS.

Further research reveals that combination of different methods such as geostatistics, spatial autocorrelation theory, multivariate statistical analysis and GIS can detect the presence of heavy metals spatial problems in a fast and more effective way on a larger scale. It was found the most appropriate way to design the samples, predict their errors along visualization. (Liang et al., 2017; Li et al., 2017) but the interpolation process works under the uncertain conditions, followed by uncertainty for the making of environmental decisions. For the sake of a certain dataset for the improvement of the spatial valuation of contaminated soils, a detailed study was carried out. In which they determined quantitatively about ambiguity and chances to adopt the heavy metals presence in the polluted zones with the help of indicators specified for the one-point and two-point stochastic site. By comparing this data with the integrated pollution index, a very informative data can be collected for the evaluation of risk at local and worldwide. A quantitative analysis were carried out (Kim et al., 2019) in which they studied briefly about high level of arsenic and lead pollution at a Korean site. Moreover, the top layer soil was taken for the in situ analysis and non-in situ analysis as well. By using ICP-AES data (primary variables) and all portable X-ray fluorescence (PXRF) data (secondary variables), some traditional kriging was done to understand the cogency about the amount of heavy metals at some non-sampled areas. The obtained results showed that PXRF gives trustworthy auxiliary dataset for improvement of spatial assessment of polluted soils, along with less expensive investigations in short period of time. At different levels and by various analysis methods, the specific features of spatial distribution of heavy metals have been determined. In which their transportation directions were focused among various countries, provinces and active areas. After penetrating to the soil, heavy metals spreads horizontally and vertically. Hence they show various spatial distribution features of pollution. It has been observed that sample taken out from soil surface, while in a horizontal direction, amount of heavy metals usually showed a gradual decline by increasing path length from the main source and vice versa for the vertical direction. Shen and his colleagues have observed that in soil layers, heavy metals surpassed optimum levels around 0 to 100 cm (Shen et al., 2017). Moreover, it was observed that heavy metals surpassed the border line and the soil surface area surrounded by the source is polluted. In last decade, different countries were taken as scales for research (Duan et al., 2016). In study, they have explored and integrated the pollution level in China's soil and found that by illustration of the basic map of china, the quantitative dispersal of heavy metals was confined in soil surface. In another study Ballabio and coworkers have studied the presence of Cu's in 25 EU Member States soil (Ballabio et al., 2018). In which it has been studied that for the better detection of the Cu amount, Gaussian Process Regression (GPR) and Kriging methods can be used together. Moreover, according to the map information, the top surface of the soil reveals about containing Cu in more efficient way, which shows that mapping helps in improving the accuracy. It has been investigated recently the presence of As, Pb, Cd, Co, Zn and Cu in the soil (Pouret et al., 2016) in the most polluted areas such as Katanga Cu belt (Democratic Republic of Congo). Purpose of this investigation was to check the effect of mining and smelting activities on the environment of this area. In Algeria, at a place of solid waste, the upper layer of soil was studied by group of scientists (Ihedioha et al., 2017). In their study, it was found that the soil layer with solid waste had most of the heavy metals as compared to the layer without solid waste. Researchers around the globe have focused on spreading of heavy metals and the resultant pollution in different areas such as the metropolises, cultivation areas and mining places along with their main sources and risk factors. It has been studied about the connection between heavy metals and their spread levels in Rizhao City, China by various scientists (Wei and Yang,

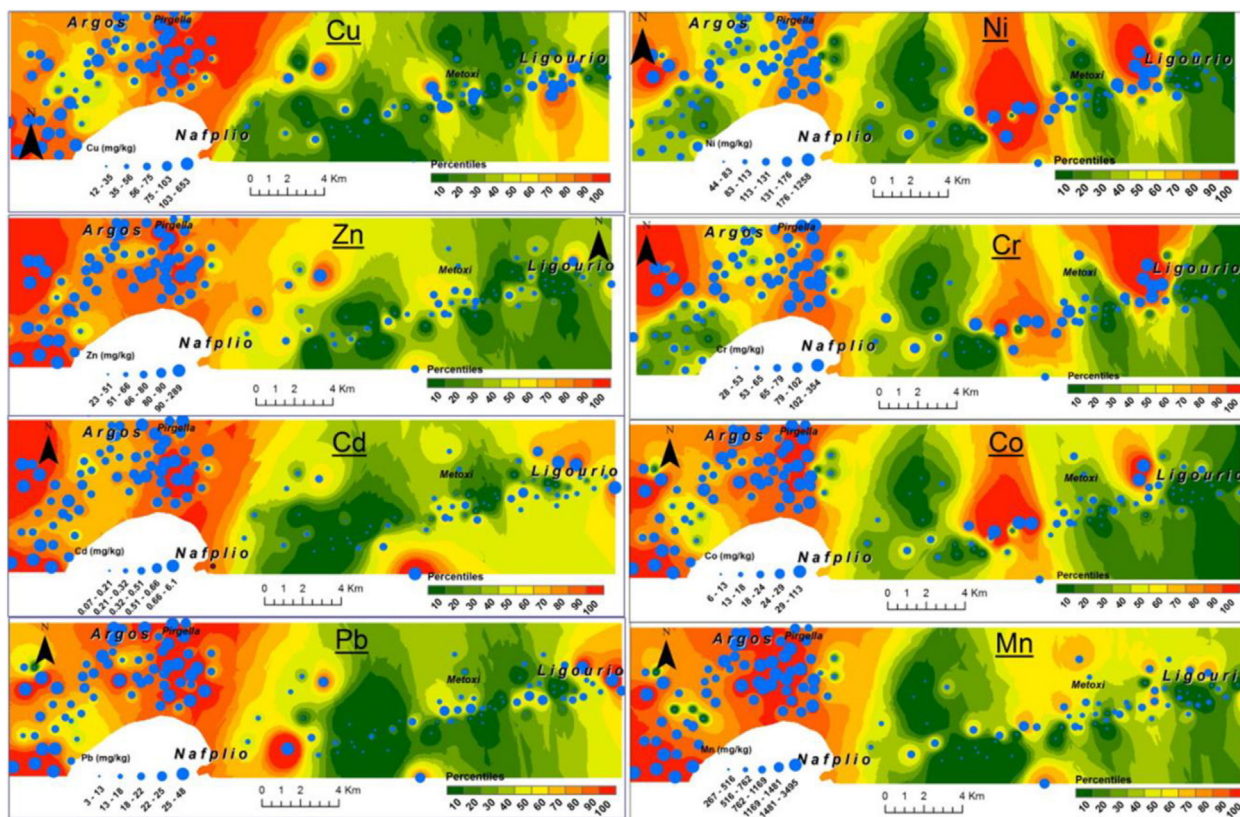


Fig. 1. Spatial layout of heavy metals in agricultural soils in the Argolida basin. Figure reprinted with permission from Elsevier, copyright 2014 (Kelepertzis, 2014).

2010; Cheng et al., 2014). Moreover, it was found the affecting scale of environmental factors and a comparison were made with previous studies as well. Which shows that in previous work, focus points were only specific areas, and assessments were made by taking samples from those selected areas only. If a careful integration could be done, then the data collected from all possible areas can help to understand the exact current condition of soil pollution. Yang et al. have done a literature survey and collected data about heavy metal contents in 402 industrial places and 1041 agricultural places (Yang et al., 2018). According to the databank, they assess the risk factors for the environment and health by soil pollution. By locating the exact existence points of heavy metals in layers of soil, scientific research has been upgraded and expanded according to requirements of pollution evaluation.

3. Synthetic approaches and heavy metal ion detection by nanomaterials

3.1. Heavy metal detection using Eco-friendly green synthetic approaches

Nanomaterials synthesized by green synthetic strategies are not hazardous for the environment as compared to the conventional methods being used up previously in labs and industries. Green synthesis methods have been involved in utilization of essential phytochemicals e.g. carboxylic acids, amides, phenols, ketones, aldehydes, flavonoids, alkaloids, ascorbic acids and various other biological components (fungi, plants, bacteria, and yeast) as reductants or protective agents (Narayanan and Sakhthivel, 2011; Yurkov et al., 2011; Marchiol, 2012; Iravani, 2014; Singh et al., 2018; Azmi et al., 2021). There are different natural backgrounds on which green synthesis depends along with several reaction conditions as solvent system pH and temp. For fabrication of metals nanopar-

ticles, phytochemicals are supposed to be the most suitable option. A green and reliable method in which extracts of lemon and oranges were used have been reported (Ravi et al., 2013). Lemon and orange extract is rich source of ascorbic and citric acid and capable of reducing the Ag and Au ion into the simple metal nanoparticles. Although, lemon and orange are considered to be the good reducing agents, but extract of lemon under the exposure of sunlight work as reducing agent for silver nanoparticles. While orange extract act as stronger reducing agent even in absence of sunlight. Instrumental studies make sure that Au and Ag NPs based on the extract of orange and lemon were more sensitive towards harmful Hg^{2+} at the micro-molar level and sensed Hg^{2+} at varied pH range (3.2–8.5). The involvement of eucalyptus globules leaf extract has also been reported (Madhavi et al., 2013; Annadhasan et al., 2014). Batch experiment was used under the controlled adsorption factor at room temperature for the removal of Cr^{6+} by zero-valent-iron nanoparticles (ZVNI) and results 98.1% adsorption capacity at dosage rate of 0.8 g/L within 30 min. However, it is important to note that stability period after synthesis was found two months for the as-prepared Fe-NPs. Moreover, Annadhasan and his colleagues have reported sensing of Pb^{2+} , Hg^{2+} , and Mn^{2+} metal ions in aqueous media by using L-tyrosine stabilized Au and Ag NPs under optimized conditions (Annadhasan et al., 2014). It has been found that the presence of OH and $-COO^-$ functional groups act as strong reducing agents for reduction of metal ion into metal NPs. But COO^- was difficult group to fit on surface of NPs. Studies have shown that AgNPs showed greater sensitivity for sensing of the different ions such as Hg^{2+} and Mn^{2+} ions at a level of 16 nM LOD. Moreover, AuNPs were found more sensitive for the detection of the Pb^{2+} and Hg^{2+} ions with 16 and 53 nM LOD. Furthermore, Liu and coworkers used the biomass for the fabrication of the branched poly ethylenimine capped fluorescent carbon quantum dots (CQDs) for the selective detection of Cu^{2+} (Liu et al., 2014). Bamboo leaves extract produced branched

polyethylenimine while preparation of CQDs carried out by capping the CQDs via electrostatic adsorption followed by their use for sensing of Cu ions present in river water. The high yield around 7.1 % were obtained by the carbon-QDs along with a 0.333 to 66.6 μM linear dynamic range with 115 nM of LOD. Ahmed and coworkers developed novel strategy for the recognition of the Hg^{2+} ions through calorimetry by approaching reduction through green synthesis and used polyethylene glycol poly vinylpropyl stabilized silver based NPs and studied by surface plasmon resonance in UV/Vis spectroscopy. (Ahmed et al., 2014) Among absorbance intensity of AgNPs, and concentration of Hg^{2+} ion, an inverse and linear relationship was found over the range of 10 to 1 ppm. But the 1 ppm LOD showed the absorption at 411 nm. Devnani and colleagues performed the evaluation of electrochemical sensing method about detection of metals via Au NPs prepared by the anthocyanin capped carbon paste electrode and black rice extraction produced anthocyanin (Devnani and Satsangee, 2015). Results showed that various metals (Cu^{2+} , Pb^{2+} and Cd^{2+}) were detected through modification of the anthocyanin capped carbon paste electrode (GNMACPE), in which a variety of surfactants and electroactive surface area was developed with 0.365 cm^2 intended for AuNPs/MACPE and found to be the most appropriate for metal ions sensing via voltammetry. Yu et al synthesized fluorescent carbon dots (water soluble) through eco-friendly hydrothermal approach with the Jinhua bergamot as source of carbon. The fabricated carbon dots possessed great stability and luminescence and act as fluorescent probe and used for detection of Hg^{2+} or Fe^{3+} ions (Fig. 2) Yu et al. (2015).

The luminescence was quenched by HAC-Na-AC for Hg^{2+} ions and Tris-HCl for the Fe^{3+} detection with low cost, quick response, specificity with wider range of 0.025 to 100 μM and 0.01 to 1000 μM along with the detection limits of 0.075 μM and 5.5 nM respectively for the Fe^{3+} and Hg^{2+} was obtained. Shi and coworkers discussed the green approach for synthesis of the oxygen-rich nitrogen-doped graphene based quantum dots (N-GQDs) for the recognition of Hg^{2+} metal ions present in the river water (Shi et al., 2015). The synthesis of N-GQDs was done via solid-phase approach by locating 3,4 dihydroxy L phenyl-alanine (L-DOPA) as citric acid. Results showed that the wavelengths about emission excitations were observed around 445 and 346 nm with 18% of the quantum yield because of the involvement of nitrogen atom to GQDs. The fabricated nitrogen-graphene-QDs fluoro-sensor was specific for the detection of Hg^{2+} due to their slaking effect of metal ions via non-radiative transfer of electrons with LOD value of 8.6 nM. Moreover, AgNPs were used to study the biopolymer Xylan which act as stabilizing and reducing agent for metal ions. Apart from this, Tollen's reaction was applied for sensing the Hg^{2+} . Studies revealed that AgNPs prepared via green methods were found to be mono-dispersed with size of >20–35 nm because

of the package of Xylan (Luo et al., 2015). Although 15 other metals were present but Hg^{2+} was detected specifically with LOD of 4.6 nM. By using xylan-Ag NPs as detecting source, some real water samples were also analyzed for the detection of Hg^{2+} . For the purpose of the surface modifications, Poly-dopamine has been applied widely because of its adhesive purposes of mussels. So, Annadhasan and Rajendiran used the AgNPs for the specific recognition of tap water Hg^{2+} ions. AgNPs was prepared by using N-cholyl-L-cysteine (NaCysC) which played role as reducing and capping agent at room conditions and sunlight exposure (Fig. 3) (Annadhasan and Rajendiran, 2015). According to the results, AgNPs showed average size of 7.8 nm. The fabricated AgNPs were used to detect the Hg^{2+} ions with LOD around 8 nM. It has been found in another study that successful detection of Hg^{2+} ions was done by AgNPs further stabilized with the help of a GMA (green multifunctional agent), and Burmese grape (fruit juice) in sonochemical condition (Annadhasan and Rajendiran, 2015). It has been observed via a comparative study that AgNPs with functional groups adsorbed on to the surface through active places on the biomolecules helped in changing the aggregation of nanomaterials. For Hg^{2+} ions, mono-dispersed AgNPs showed a size range between 5 and 10 nm with 47.6 μM LOD at varied pH (3.73–11.18). Similarly, detection of Ni^{2+} and Co^{2+} ions inside water, via calorimetric method was made by the N cholyl-L-valine (Na-ValC)-reduced gold nanoparticles (AuNPs) without exposure of the sunlight (Annadhasan et al., 2015). The variations in size and shape of the Na-ValC-capped AuNPs was noticed by changing the concentrations. Lower concentration gave the AuNPs average size around 40 nm and higher concentration provides 8.0 nm size. Moreover, in Na-ValC the functional groups $\text{NH}-\text{C}=\text{O}$ and OH took part in metal ions reduction, while for the stabilization of these AuNPs hydrophilic and lipophilic moieties were involved. The coefficient of linear regression (R^2) and LOD the were exist around 10 nM and 0.9870 for Ni^{2+} while 10 nM and 0.9806 for Cu^{2+} ions, respectively. Nitrogen-doped based carbon dots were prepared by using a lotus root which acted as carbon source (Gu et al., 2016). For the production of the CDs, lotus root was found to be the best choice due to presence of polysaccharides, alkaloids, glycoprotein and amino acids, act as a source for the carbon and nitrogen. One pot microwave treatment results the CDs with 5.23% nitrogen content via LR by using the fluorescent nitrogen-doping, which helped as a surface passivating agent and controlled the participation of other passivating type agents. Maximum yield of 19.0% was observed by the nitrogen-capped CDs. A great level of detection was observed by LR carbon dots for the Hg^{2+} ions with LOD of 18.7 nM. It was found after study that detection of metal ions via calorimetry is very easy and it can observe via naked eye as well (Cheon and Park, 2016). AgNPs by using mussel-inspired protein also helped to detect the Pb^{2+} and Cu^{2+} ion successfully via colorimetric

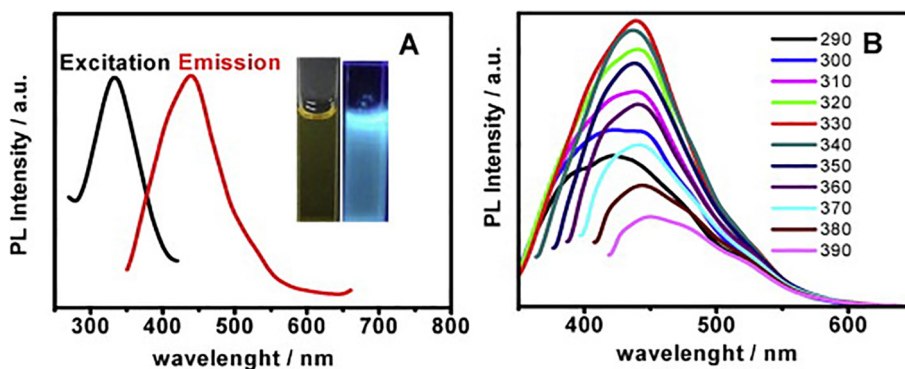


Fig. 2. (A) Fluorescence excitation (black line) and emission (red line) spectra of C-dots. Inset shows C-dots under visible light (right) and 365 nm UV light (left). (B) The corresponding emission spectra of C-dots at different excitation wavelength from 290 to 390 nm. Reproduce with permission from (Yu et al. 2015).

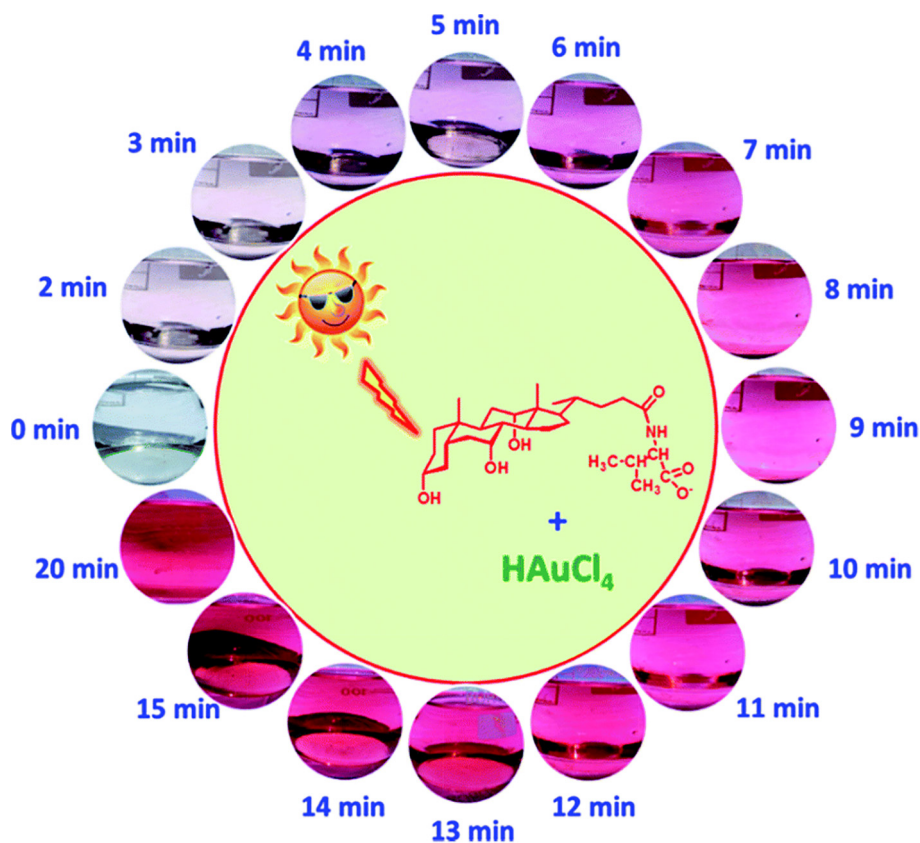


Fig. 3. Schematic illustration of AuNPs formation at different time intervals under natural sunlight irradiation. Figure reprinted from Ref. [Annadhasan and Rajendiran, \(2015\)](#) with permission from RSC, copyright 2015.

method. In this case, AgNPs are synthesized and 3,4 dihydroxy L-phenyl-alanine (poly DOPA) was found involved for stabilization and reduction purpose and results showed that as-synthesized poly DOPA-AgNPs has the size 25 nm with higher dispersion. TEM images showed that accumulation of the poly DOPA-AgNPs resulted the change in color from yellow to brown and LOD of 9.4×10^{-5} and 8.1×10^{-5} M for Pb^{2+} and Cu^{2+} ions. Similarly, detection of Hg^{2+} and Fe^{2+} ions takes place via calorimetric method, for this purpose sugar bodies (dextrose and maltose) reduced AgNPs were used ([May and Oluwafemi, 2016](#)). The change in size of the sugar-reduced gelatin-capped AgNPs was observed. For maltose and dextrose-capped AgNPs, the size was found to be 11.88 and 18.17 nm, respectively. It was observed that dextrose-reduced NPs showed more sensitivity for the detection of the metal ions as compared to the maltose at higher level of metal ions. Maltose and dextrose-reduced AgNPs detected the Hg^{2+} and Fe^{2+} ions at 0.001 M and 0.1 M respectively and showed higher sensitivity for the Hg^{2+} ions up to 10^{-12} M with a linear range of 10^{-1} to 10^{-5} M. Novel method by using the egg white capped AgNPs for the sensing of Hg^{2+} ions in water have been explored. ([Tirado-Guizar et al., 2017](#)) It was found that egg white showed great activity for the preparation of the AgNPs with increased specific binding positions for the Hg^{2+} ions related to the attachment of the thiol groups. AgNPs with egg white capping showed specificity for sensing of the Hg^{2+} ions in the existence of various other metals with the limit of detection of 300 nM Generally, Hg^{2+} ions detection was made by the calorimetric method via green synthesized AgNPs. AgNPs were prepared by using fruit extract such as *Carica papaya* in the exposure of sunlight ([Firdaus et al., 2017](#)). For the oxidation of metal ions into the zero oxidation state, ascorbic acid and phenolics are involved and bio-active compounds (water-soluble) extracted from the papaya fruit served as the bio-

reductants of Ag^{1+} to form Ag NPs and Hg^{2+} ions were detected specifically in the presence of other metals. Furthermore, more attraction was governing by AgNPs for the Hg^{2+} ions and it was observed from the colorimetric results that the Hg^{2+} ions changed the solution color from yellowish brown to the colorless. Disappearance of color takes place because of oxidation of silver metal in AgNPs to Ag^{1+} .

3.2. Heavy metal detection using chemical synthetic approaches

Mono-dispersed nanomaterials have been produced using a variety of chemical and physical techniques, e.g., phytochemical ([Narchin et al., 2018](#)) electrochemical ([Singaravelan and Alwar, 2015](#)), laser ablation ([Sadrolhosseini et al., 2019](#)), co-precipitation ([Kandpal et al., 2014](#)) and arc discharge ([El-Khatib et al., 2018](#)) techniques. These traditional synthesis techniques can simply harvest smaller and more uniform nanoparticles. Prior to high surface to volume ratio and excellent functionalities of nanomaterials, physical and chemical synthesis techniques were often employed for heavy metal recognition. Herein, Yang and colleagues fabricated Bi-NPs for selective and sensitive recognition of Cd^{2+} and Pb^{2+} ions. Reduction of Pb^{2+} and Cd^{2+} by employing Bi-NPs based modified glassy carbon electrode (GCE) provided an obvious response at 0.85 V and 0.65 V respectively. Bi-NPs found to be highly selective with detection limit of 10 g/L for Pb^{2+} and Cd^{2+} and a small particle size distribution of about 80 nm ([Yang et al., 2013](#)). Another study discovered the use of carbon xerogel Bi-NPs for recognition of lead and Cadmium ions in an electro-chemical experiment ([Gich et al., 2013](#)). The electrochemical performance of the synthesized NPs was achieved with low LOD (<1 ppb) for Pb and Cd in aqueous system. By employing the square wave anodic stripping voltammetry, Zhu and coworkers investigated the

determination of Pb^{2+} and Cd^{2+} ions through Au-NPs graphene cysteine composite with glassy carbon electrode (Zhu et al., 2014). Because of the electrical conductivity and synergetic effect of Au-NPs combined with cysteine and graphene, the deposition of Cd^{2+} and Pb^{2+} ions on modified glassy carbon electrodes was critical. The LOD of Cd^{2+} (0.10 g/L) and Pb^{2+} (0.05 g/L) was found to be very low, with a linear relationship between current and Cd^{2+} and Pb^{2+} concentrations ranging from 40 to 0.50 g/L. Alternatively, for the colorimetric detection of Hg^{2+} ions, SiO@Ag core-shell NPs were used (Boken and Kumar, 2014). Chemical reduction synthesis technique was used to fabricate SiO@Ag core-shell NPs, which had a surface plasmon resonance peak at 433 nm for the Ag-NPs and 450 nm for Ag core-shell and NPs and these were found enormously sensitive to Hg^{2+} in aqueous medium with low detection limit. As synthesized Ag-NPs had shell thicknesses of 28 nm and sizes of 202 nm. Heavy metals such as Pb^{2+} , Ni^{2+} and Cd^{2+} were successfully determined using a carbon paste electrode designed with Bi-NPs in an electrochemical test (Niu et al., 2015). In different water samples (ground polluted and tap water), the Bi-NPs based electrochemical sensor exhibited excellent sensitivity and selectivity for Ni^{2+} , Pb^{2+} , and Cd^{2+} and revealed a very low detection limit of 5.47 ppb for Ni^{2+} , 0.65 ppb for Pb^{2+} , and 0.81 ppb for Cd^{2+} ions. Graphene and quantum dots have been broadly utilized in numerous sensing fields due to their remarkable physicochemical properties. Using an electrochemical detection method, Au-NPs-graphene quantum dots (GQDs) were developed for selective recognition of Cu^{2+} and Hg^{2+} ions (Fig. 4) (Ting et al., 2015). Because of the smaller narrow particle size 50 nm of Au-GQDS, these are found highly sensitive to Cu^{2+} and Hg^{2+} ions with ultra-low detection limits of 0.02 nM for Hg^{2+} and 0.05 nM for Cu^{2+} ions. For the detection of Pb^{2+} ions in an electrochemical system decorated glassy carbon electrodes with ferrite $MnFe_2O_4$ NPs in a mesoporous cluster arrangement have been used (Han et al., 2015). This electrode architecture strategy detected the Pb^{2+} with a low LOD of 0.054 nM under appropriate electrochemical parameters. The size of as-prepared $MnFe_2O_4$ NPs was found between 200 and 400 nm with mesoporous nature and a diameter of 8 to 12 nm. Also, Xie and co-workers described graphene/CeO₂ based hybrid material for determination of Cu^{2+} , Hg^{2+} , Pb^{2+} and Cd^{2+} metal ions

(Xie et al., 2015). By using a hydrothermal process, cerium oxide nanoparticles with graphene hybrid caps were fabricated and integrated onto a GCE. According to the findings, as-prepared graphene/CeO₂ hybrid materials were highly selective and responsive to Cd^{2+} , Hg^{2+} , Cu^{2+} and Pb^{2+} ions. The reported LOD was significantly lower than the World Health Organization's (WHO) recommended values. On the other hand, Sulistiawaty et al. assessed Tween-20 and gelatin as a stabilizing agent for colorimetric detection of Hg^{2+} ions through Ag-NPs (Sulistiawaty et al., 2015). Hg^{2+} metal ions were noticed to be very selective for Tween-20 and gelatin stabilized Ag-NPs with low LODs for gelatin AgNPs (0.45 mg/L) and Tween-20 (0.13 mg/L). Tween-20 Ag-NPs had a diameter of 17.54 nm, while gelatin AgNPs had a diameter of about 9.68 nm. Iron oxide nanoparticles (Fe₂O₃ NPs) have been (Bobik et al., 2015) exploited for the adsorption of different heavy metal such as Ni^{2+} , Cu^{2+} , Zn^{2+} , Cd^{2+} , Cr^{3+} , Pb^{2+} and Cr^{4+} ions. Fe₂O₃ NPs were prepared using co-precipitation technique at various temperatures and ammonia volumes resulting in different adsorption capacities for Ni^{2+} , Cu^{2+} , Zn^{2+} , Cd^{2+} , Cr^{3+} , Pb^{2+} and Cr^{4+} ions. Multicomponent-NPs (MCNPs) were used for 99% elimination of As, Ag, Pb and Cu metal ions from the artificial mine tailing (Stael and Cumbal, 2016). To make MCNPs, researchers used a novel synthesis technique and employed nitrogenized water to synthesize different concentrations of Na₂SO₄, NaBH₄, and FeCl₃. Within 5 min, the As, Ag, Pb and Cu metal ions were removed more than 99.50%. Likewise, Shi and colleagues established an electrochemical valuation for the synchronized determination of Pb^{2+} , Cd^{2+} and Zn^{2+} ions by using 3D graphene-framework-Bi NPs (Fig. 5) (Shi et al., 2017). The tunable morphologies of Bi-NPs were reduced electrochemically and widely distributed on the framework and providing broad active surface area for heavy metal detection. 3D graphene-framework-Bi-NPs were remarkably sensitive towards Pb^{2+} , Cd^{2+} and Zn^{2+} ions metal ions (Bobik et al., 2015) and LODs were detected as 0.02 µg/L for Pb^{2+} ; 0.05 µg/L for Cd^{2+} and 300 µg/L for Zn^{2+} ions. Furthermore, Zhou and colleagues used L-cysteine functionalized $MnFe_2O_4$ -glassy carbon electrode to detect different (Cu^{2+} , Cd^{2+} , Pb^{2+} and Hg^{2+}) metal ions in a sensitive and selective manner. Under individual and simultaneous detection conditions, $MnFe_2O_4$ /Cysglassy carbon electrodes were extremely sensitive to Pb^{2+} ions, with high sensitivity of 57.0 and 35.3 µA/µM. (Zhou et al., 2017). Cu-reduced graphene oxide (CuNPs/RGO) were synthesized through the liquid-phase reduction to electrochemically estimate different heavy metal ions (Cu^{2+} , Hg^{2+} , Cd^{2+} and Pb^{2+}) (Li et al., 2017). CuNPs/RGO were used to detect metal ions simultaneously using cyclic voltammetry (CV) and electrochemical impedance spectroscopy (EIS). The findings established that synthesized nanocomposites were greatly sensitive to metal ions, with limit of detection values of 0.111 nM for Cu^{2+} , 0.051 nM for Hg^{2+} , 0.203 nM for Cd^{2+} and 0.186 nM for Pb^{2+} ions. Sarkar and his colleagues developed a colorimetric procedure for measuring Hg^{2+} ions in collected water sample by a model extremely efficient mercury sensor (Sarkar et al., 2017). A low-cost prototype mercury sensor based on Ag-NPs impregnated with poly vinyl alcohol (PVA-AgNPs) was used to recognize Hg^{2+} ions with LOD value of 10 ppb. Surface plasmon resonance band of silver based nanoparticles were lost due to the aggregation and amalgamation with the Hg^{2+} ions and yellowish colour of solution turns to colorless in existence of mercury ions. Glassy carbon electrode modified with use carbon NPs was used for the selective and sensitive determination of heavy metals including Cu^{2+} , Pb^{2+} and Hg^{2+} ions in aqueous media (Fig. 6) (Simpson et al., 2018). Three separate reducing sources were used to make the carbon-NPs, such as (1) glycerol and silica, (2) glycerol and H₃PO₄, and (3) glycerol, H₃PO₄, and silica. The size distribution of the as-synthesized carbon-NPs was 89 nm, 66 nm, and 58 nm. Carbon-NPs based electrode was enormously sensitive with detection limits of Cu^{2+}

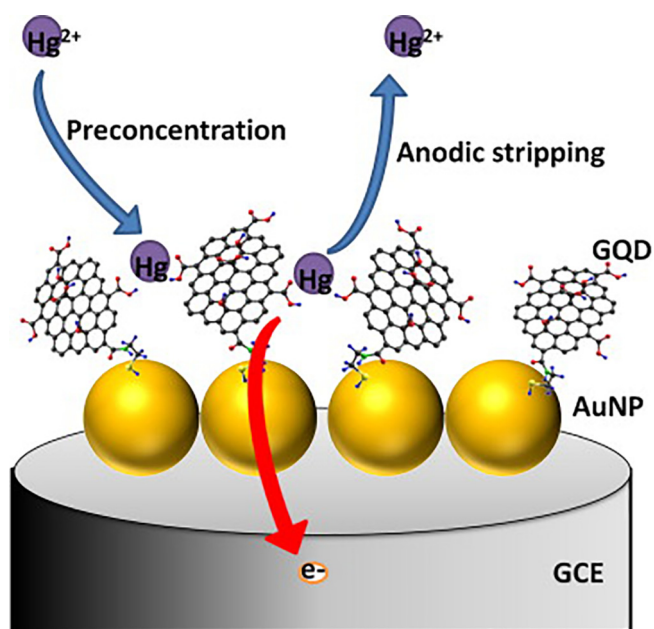


Fig. 4. Schematic illustration of Hg^{2+} detection. Figure reprinted from Ref. Ting et al. (2015) with permission from Elsevier, copyright 2015

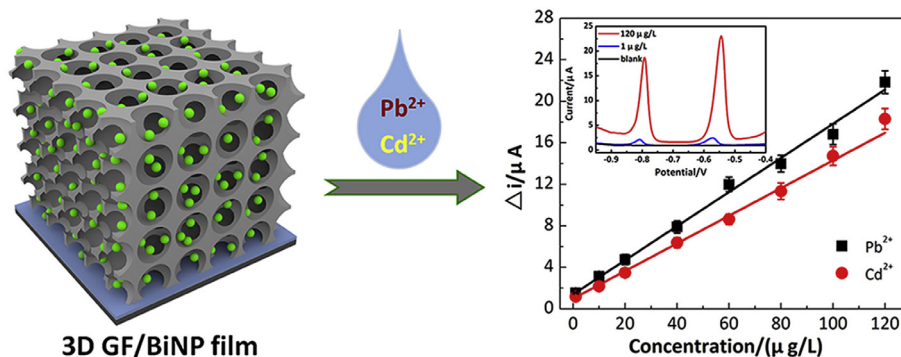


Fig. 5. Schematic illustration of Facile fabrication of a novel 3D graphene framework/Bi nanoparticle film for ultrasensitive electrochemical assays of heavy metal ions. Figure reprinted from Ref. Shi et al. (2017) with permission from Elsevier, copyright 2017.

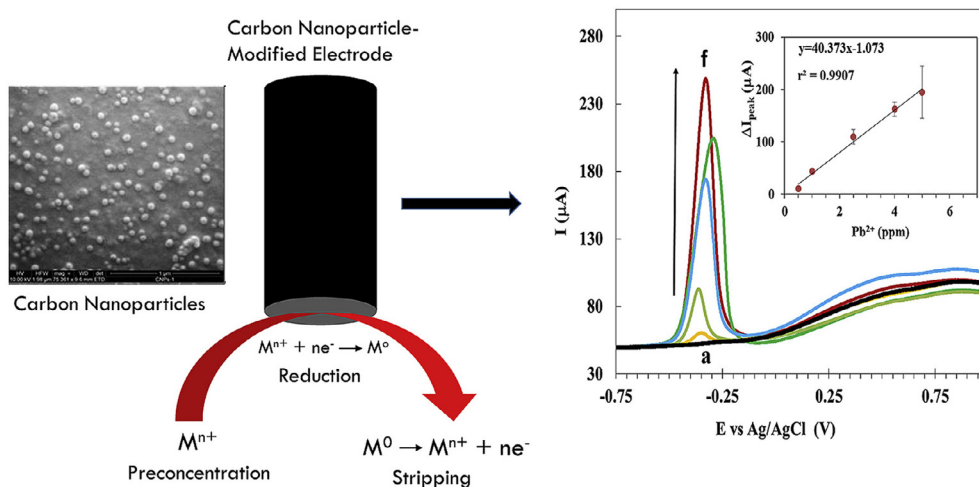


Fig. 6. Schematic Illustration of synthetic and detection processes of carbon nanoparticles for heavy metal ions in aqueous media. Figure reprinted from Ref. Simpson et al. (2018) with permission from Elsevier, copyright 2018.

0.50 ppm, Hg^{2+} 31 ppm and Pb^{2+} 0.30 ppm respectively. However, Zhou and coworkers established another electrochemical assay to selectively recognize the Pb^{2+} ions with ferrite-NPs (MnFe_2O_4) incorporated with graphene oxide (Zhou et al., 2018). The GO/ MnFe_2O_4 nanocomposites were uniform in size, having diameter in the range of 400 nm and porosity of 4.5 nm. GO/ MnFe_2O_4 presented promising sensitivity to Pb^{2+} ions with LOD value of 0.0883 μM . Furthermore, Antunović and colleagues identified an electrochemical pathway for instantaneous detection of Pb^{2+} and Cd^{2+} metal ions using MnCo_2O_4 NPs modified bare glassy carbon electrode. MnCo_2O_4 NPs were synthesized using the citrategel combustion method and instrumental findings exhibited that NPs were mono-dispersed with a size distribution of 19 nm. LOD was found to be 8.06n mol/dm³ for Pb^{2+} ions and 7.02 nmol/dm³ for Cd^{2+} ions, respectively (Antunović et al., 2019). Cu-NPs were used to detect Ag^{2+} ions colorimetrically in the aqueous medium. Cu-NPs were found to be uniformed in size with diameter of 5.0 nm. The Cu-NPs showed good selectivity for Ag^{2+} ions with wide linear range (100–600 mol/L) (Wang et al., 2019).

4. Conclusion and prospects

Conclusively, efforts to build nanomaterials-based sensors for heavy metal detection were examined in order to increase sensitivity, selectivity, and overall device performance. Furthermore, improved selectivity and sensitivity in detecting of these heavy

metals have been accomplished by integrating nanomaterials in the architecture of sensors. When compared to traditional approaches such as fluorescent sensors, ICPOES, AAS, AES, ICP-MS etc. the nanosensors based on functionalized NPs offer various advantages. Nanomaterial-based sensors, which are made from stable, biocompatible, affordable, and nontoxic inorganic chemicals, are preferred over conventional sensors because of their high low cost, LOD, and convenience of use for in-field applications. Additionally, the use of nanomaterials as detection materials has comprehended improvement in the on-site detection ability sensitivity, portability, selectivity, and overall performance of the detecting systems. Though gigantic innovations and advances have been perceived, but the recognition of these heavy metal ions with nanosensors still facing great developmental challenges related with their applications in real-world samples including biological and raw water samples. The delusional self-stability of nanomaterials must be addressed to meet the requirement for heavy metal ions sensing in complex matrices such as seawater, wastewater, and biological samples. As a result, innovative stable nanomaterials must be designed and developed, necessitating the use of novel modification techniques for enhanced functionalization. In addition, the selectivity of the nanomaterial based sensor can be enhanced by employing biological molecules or small molecule based ligands as detection sites in the architecture of nanomaterial derived sensor. The binding site or recognition unit can facilitate the chemical or biological interaction with the analyte which will allow the selective sensing of heavy metals. Finally, combining

nano systems with other technologies such as test strips or paper chips, as well as microfluidic, holds a lot of potential for the production of smart devices to monitor heavy metal ions on industrial or commercial scale.

Declaration of Competing Interest

The authors declare that they have no known competing financial interests or personal relationships that could have appeared to influence the work reported in this paper.

Acknowledgment

The authors sincerely appreciate funding from Researchers Supporting Project number (RSP-2021/58), King Saud University, Riyadh, Saudi Arabia.

References

- Ahmed, M.A., Hasan, N., Mohiuddin, S., 2014. *Int. Schol. Res. Notices* 2014.
- Annadhasan, M., Rajendiran, N., 2015. *RSC Adv.* 5, 94513–94518.
- Annadhasan, M., Muthukumarasamyvel, T., Sankar Babu, V., Rajendiran, N., 2014. *ACS Sustainable Chem. Eng.* 2, 887–896.
- Annadhasan, M., Kasthuri, J., Rajendiran, N., 2015. *RSC Adv.* 5, 11458–11468.
- Antunović, V., Ilić, M., Baošić, R., Jelić, D., Lolić, A., 2019. *PLoS One* 14, e0210904.
- Azmi, S.N.H., Iqbal, B., Al Khanbashi, R.S., Al Hamhami, N.H., Rahman, N., 2013. *Environ. Monit. Assess.* 185, 4647–4657.
- Azmi, S.N.H., Al-Balushi, M., Al-Siyabi, F., Al-Hinai, N., Khurshid, S., 2020. *J. King Saud Univ.-Sci.* 32, 2931–2938.
- Azmi, S.N.H., Al-Jassasi, B.M.H., Al-Sawafi, H.M.S., Al-Shukaili, S.H.G., Rahman, N., Nasir, M., 2021. *Environ. Monit. Assess.* 193, 1–16.
- Azmi, S.N.H., Iqbal, B., Al Ruqishi, B.H.K., Al Sayabi, S.A.M., Al Quraini, N.M.K., Rahman, N., 2016. *J. Assoc. Arab Univ. Basic Appl. Sci.* 19, 29–36.
- Ballabio, C., Panagos, P., Lugato, E., Huang, J.-H., Orgiazzi, A., Jones, A., Fernández-Ugalde, O., Borrelli, P., Montanarella, L., 2018. *Sci. Total Environ.* 636, 282–298.
- Bobik, M., Korus, I., Brachmańska, M., 2015. *Proceed. ECOPELE* 9.
- Boken, J., Kumar, D., 2014. *Int. J. Environ. Res. Dev.* 4, 303–308.
- Borah, S.B., Bora, T., Baruah, S., Dutta, J., 2015. *Groundwater Sustainable Dev.* 1, 1–11.
- Boruah, P.K., Das, M.R., 2020. *J. Hazard. Mater.* 385, 121516.
- Cheng, H., Li, M., Zhao, C., Li, K., Peng, M., Qin, A., Cheng, X., 2014. *J. Geochem. Explor.* 139, 31–52.
- Cheon, J.Y., Park, W.H., 2016. *Int. J. Mol. Sci.* 17, 2006.
- Devnani, H., Satsangee, S., 2015. *Int. J. Environ. Sci. Technol.* 12, 1269–1282.
- Duan, Q., Lee, J., Liu, Y., Chen, H., Hu, H., 2016. *Bull. Environ. Contam. Toxicol.* 97, 303–309.
- El-Khatib, A.M., Badawi, M.S., Ghatass, Z., Mohamed, M., Elkhatib, M., 2018. *J. Cluster Sci.* 29, 1169–1175.
- Firdaus, M., Andriana, S., Elvinawati, Alwi, W., Swistoro, E., Ruyani, A., Sundaryono, A., 2017. Green synthesis of silver nanoparticles using Carica Papaya fruit extract under sunlight irradiation and their colorimetric detection of mercury ions. *J. Phys. Conf. Ser.* 817, 012029.
- Gaiss, S., Amarasiriwardena, D., Alexander, D., Wu, F., 2019. *Environ. Pollut.* 252, 657–665.
- García-Carmona, M., Romero-Freire, A., Aragón, M.S., Garzón, F.M., Peinado, F.M., 2017. *J. Environ. Manage.* 191, 228–236.
- Ghadermazi, J., Sayyad, G., Mohammadi, J., Moezzi, A., Ahmadi, F., Schulin, R., 2011. *Proc. Environ. Sci.* 3, 130–135.
- Gich, M., Fernández-Sánchez, C., Cotet, L.C., Niu, P., Roig, A., 2013. *J. Mater. Chem. A* 1, 11410–11418.
- Gu, D., Shang, S., Yu, Q., Shen, J., 2016. *Appl. Surf. Sci.* 390, 38–42.
- Han, X.-J., Zhou, S.-F., Fan, H.-L., Zhang, Q.-X., Liu, Y.-Q., 2015. *J. Electroanal. Chem.* 755, 203–209.
- Ihedioha, J., Ukoha, P., Ekere, N., 2017. *Environ. Geochem. Health* 39, 497–515.
- Iravani, S., 2014. *Int. Schol. Res. Notices* 2014.
- Jang, C.-S., Liu, C.-W., Lu, K.-L., Lin, C.-C., 2007. *Environ. Monit. Assess.* 134, 293.
- N. Kandpal, N. Sah, R. Loshali, R. Joshi, J. Prasad, (2014).
- Kanwar, V.S., Sharma, A., Srivastav, A.L., Rani, L., 2020. *Environ. Sci. Pollut. Res.*, 1–26
- Kaur, B., Srivastava, R., Satpati, B., 2015. *New J. Chem.* 39, 5137–5149.
- Kelepertzis, E., 2014. *Geoderma* 221, 82–90.
- Kim, H.-R., Kim, K.-H., Yu, S., Moniruzzaman, M., Hwang, S.-I., Lee, G.-T., Yun, S.-T., 2019. *Geoderma* 341, 26–38.
- Li, D., Wang, C., Zhang, H., Sun, Y., Duan, Q., Ji, J., Zhang, W., Sang, S., 2017. *Int. J. Electrochem. Sci* 12, 10933–10945.
- Li, X., Yang, H., Zhang, C., Zeng, G., Liu, Y., Xu, W., Wu, Y., Lan, S., 2017. *Chemosphere* 170, 17–24.
- Liang, J., Zhong, M., Zeng, G., Chen, G., Hua, S., Li, X., Yuan, Y., Wu, H., Gao, X., 2017. *Sci. Total Environ.* 579, 1675–1682.
- Lin, T., Zhong, L., Wang, J., Guo, L., Wu, H., Guo, Q., Fu, F., Chen, G., 2014. *Biosens. Bioelectron.* 59, 89–93.
- Liu, Y., Zhao, Y., Zhang, Y., 2014. *Sens. Actuators, B* 196, 647–652.
- Luo, Y., Shen, S., Luo, J., Wang, X., Sun, R., 2015. *Nanoscale* 7, 690–700.
- Madhavi, V., Prasad, T., Reddy, A.V.B., Reddy, B.R., Madhavi, G., 2013. *Spectrochim. Acta Part A: Mol. Biomol. Spectr.* 116, 17–25.
- Marchiol, L., 2012. *Ital. J. Agronomy.* e37–e37.
- May, B., Oluwafemi, O.S., 2016. *Int. J. Electrochem. Sci* 11, 8096–8108.
- Nabeel, F., Rasheed, T., 2020. *J. Hazard. Mater.* 388, 121757.
- Narayanan, K.B., Sakthivel, N., 2011. *J. Hazard. Mater.* 189, 519–525.
- Narchin, F., Larjani, K., Rustaiyan, A., Ebrahimi, S.N., Tafvizi, F., 2018. *Adv. Pharm. Bull.* 8, 235.
- Niu, P., Fernández-Sánchez, C., Gich, M., Ayora, C., Roig, A., 2015. *Electrochim. Acta* 165, 155–161.
- Pourret, O., Lange, B., Bonhoure, J., Colinet, G., Decrée, S., Mahy, G., Séleck, M., Shutcha, M., Faucon, M.-P., 2016. *Appl. Geochem.* 64, 43–55.
- Rahman, N., Azmi, S.N.H., Wu, H.-F., 2006. *Accred. Qual. Assur.* 11, 69–74.
- Rasheed, T., Nabeel, F., 2019. *Coord. Chem. Rev.* 401, 213065.
- Rasheed, T., Bilal, M., Nabeel, F., Iqbal, H.M.N., Li, C., Zhou, Y., 2018. *Sci. Total Environ.* 615, 476–485.
- Rasheed, T., Li, C., Zhang, Y., Nabeel, F., Peng, J., Qi, J., Gong, L., Yu, C., 2018. *Sens. Actuators, B* 258, 115–124.
- Rasheed, T., Li, C., Bilal, M., Yu, C., Iqbal, H.M.N., 2018. *Sci. Total Environ.* 640–641, 174–193.
- Rasheed, T., Nabeel, F., Li, C., Zhang, Y., 2019. *J. Mol. Liq.* 274, 461–469.
- Rasheed, T., Nabeel, F., Shafi, S., Bilal, M., Rizwan, K., 2019. *J. Mol. Liq.* 296, 111966.
- Rasheed, T., Nabeel, F., Adeel, M., Rizwan, K., Bilal, M., Iqbal, H.M.N., 2019. *J. Mol. Liq.* 292, 111425.
- Rasheed, T., Hassan, A.A., Kausar, F., Sher, F., Bilal, M., Iqbal, H.M.N., 2020. *TrAC Trends Anal. Chem.* 132, 116066.
- Ravi, S.S., Christena, L.R., SaiSubramanian, N., Anthony, S.P., 2013. *Analyst* 138, 4370–4377.
- Sadrolhosseini, A.R., Mahdi, M.A., Alizadeh, F., Rashid, S.A., 2019. Laser ablation technique for synthesis of metal nanoparticle in liquid. *IntechOpen.*
- Sarkar, P.K., Halder, A., Polley, N., Pal, S.K., 2017. *Water, Air, Soil Pollut.* 228, 314.
- Sarkar, B., Mandal, S., Tsang, Y.F., Kumar, P., Kim, K.-H., Ok, Y.S., 2018. *Sci. Total Environ.* 612, 561–581.
- Shen, F., Liao, R., Ali, A., Mahar, A., Guo, D., Li, R., Xining, S., Awasthi, M.K., Wang, Q., Zhang, Z., 2017. *Ecotoxicol. Environ. Saf.* 139, 254–262.
- Shi, L., Li, Y., Rong, X., Wang, Y., Ding, S., 2017. *Anal. Chim. Acta* 968, 21–29.
- Shi, B., Zhang, L., Lan, C., Zhao, J., Su, Y., Zhao, S., 2015. *Talanta* 142, 131–139.
- Simpson, A., Pandey, R., Chusuei, C.C., Ghosh, K., Patel, R., Wanekaya, A.K., 2018. *Carbon* 127, 122–130.
- Singaravelan, R., Alwar, S.B.S., 2015. *Appl. Nanosci.* 5, 983–991.
- Singh, J., Dutta, T., Kim, K.-H., Rawat, M., Samddar, P., Kumar, P., 2018. *J. Nanobiotechnol.* 16, 84.
- Stael, C., Cumbal, L., 2016. *Biol. Med.* 8, 1.
- St-Jean, A., Suhas, E., De Pina, J.-J., Cordier, S., Lucas, M., Ayotte, P., 2019. *Sci. Total Environ.* 695, 133791.
- Sulistiawaty, L., Sugiarti, S., Darmawan, N., 2015. *Indon. J. Chem.* 15, 1–8.
- Ting, S.L., Ee, S.J., Anantharayanan, A., Leong, K.C., Chen, P., 2015. *Electrochim. Acta* 172, 7–11.
- Tirado-Guizar, A., Rodriguez-Gattorno, G., Paraguay-Delgado, F., Oskam, G., Pina-Luis, G.E., 2017. *MRS Commun.* 7, 695–700.
- Trujillo-González, J.M., Torres-Mora, M.A., Keesstra, S., Brevik, E.C., Jiménez-Ballesta, R., 2016. *Sci. Total Environ.* 553, 636–642.
- Wang, N., Ga, L., Jia, M., Ai, J., 2019. *J. Nanomater.* 2019.
- Wei, B., Yang, L., 2010. *Microchem. J.* 94, 99–107.
- Xie, Y.-L., Zhao, S.-Q., Ye, H.-L., Yuan, J., Song, P., Hu, S.-Q., 2015. *J. Electroanal. Chem.* 757, 235–242.
- Yang, H., Li, J., Lu, X., Xi, G., Yan, Y., 2013. *Mater. Res. Bull.* 48, 4718–4722.
- Yang, Q., Li, Z., Lu, X., Duan, Q., Huang, L., Bi, J., 2018. *Sci. Total Environ.* 642, 690–700.
- Yao, X.-P., Fu, Z.-J., Zhao, Y.-G., Wang, L., Fang, L.-Y., Shen, H.-Y., 2012. *Talanta* 97, 124–130.
- Yu, J., Song, N., Zhang, Y.-K., Zhong, S.-X., Wang, A.-J., Chen, J., 2015. *Sens. Actuators, B* 214, 29–35.
- Yurkov, A.M., Kemler, M., Begerow, D., 2011. *PLoS One* 6, e23671.
- Zhang, Y., Zhou, H., Zhang, Z.-H., Wu, X.-L., Chen, W.-G., Zhu, Y., Fang, C.-F., Zhao, Y.-G., 2017. *J. Chromatogr. A* 1489, 29–38.
- Zhang, Y., Zhao, Y.-G., Muhammad, N., Ye, M.-L., Zhu, Y., 2020. *J. Chromatogr. A* 1618, 460891.
- Zhao, Y.-G., Zhang, Y., Wang, F.-L., Zhou, J., Zhao, Q.-M., Zeng, X.-Q., Hu, M.-Q., Jin, M.-C., Zhu, Y., 2018. *Talanta* 185, 411–418.
- Zhou, S.-F., Wang, J.-J., Gan, L., Han, X.-J., Fan, H.-L., Mei, L.-Y., Huang, J., Liu, Y.-Q., 2017. *J. Alloy. Compd.* 721, 492–500.
- Zhou, S.-F., Han, X.-J., Fan, H.-L., Huang, J., Liu, Y.-Q., 2018. *J. Alloy. Compd.* 747, 447–454.
- Zhu, L., Xu, L., Huang, B., Jia, N., Tan, L., Yao, S., 2014. *Electrochim. Acta* 115, 471–477.